ACS APPLIED MATERIALS & INTERFACES

Research Article

www.acsami.org

Bioinspired Design and Assembly of Layered Double Hydroxide/Poly(vinyl alcohol) Film with High Mechanical Performance

Yingqi Shu,[†] Penggang Yin,*[,‡] Benliang Liang,[‡] Hao Wang,[†] and Lin Guo[‡]

[†]The College of Materials Science and Engineering, Beijing University of Technology, Beijing 100124, P. R. China

[‡]School of Chemistry and Environment, Beihang University, Beijing 100191, P. R. China

ABSTRACT: Inspired by the hierarchical structure and excellent mechanical performance of nacre, LDH nanosheets with an appropriate aspect ratio to withstand significant loads and at the same time allow for rupture under the pull-out mode were synthesized as artificial building blocks for the fabrication of nacre-like films. Multilayered PVA/LDH films with a high tensile strength and ductility were prepared for the first time by bottom-up layer-by-layer assembly of pretreated LDH nanosheets and spin-coating of PVA. The weight fraction of inorganic LDH platelets in the hybrid PVA/LDH films (w_p) was controlled by changing the concentration of PVA solution applied in the spin-coating process. The resulting films revealed that the PVA/LDH hybrid films were piled close together to form a well-defined stratified structure resembling the brick-and-mortar structure of natural nacre. In the hybrid films, the content of inorganic LDH platelets was comparable to the value in nacre, up to 96.9 wt %. It could be clearly seen that the mechanical performance of the as-prepared PVA/LDH films was greatly improved by increasing the rigid building-block LDHs. The tensile strength of the 2 wt % PVA/LDH hybrid film reached a value of 169.36 MPa, thus exceeding the strength of natural nacre and reaching 4 times that of a pure PVA film. Meanwhile, its elastic modulus was comparable to that of lamellar bone.

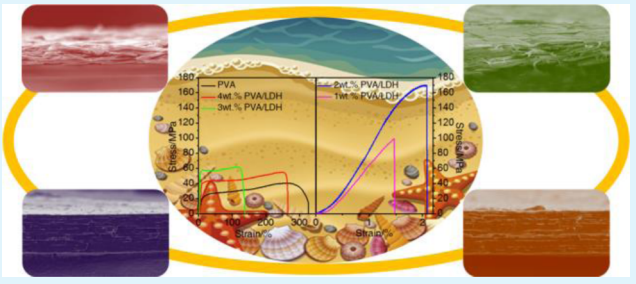

KEYWORDS: *bioinspired design, poly(vinyl alcohol), layered double hydroxide, interfacial adhesion, mechanical properties*

INTRODUCTION

During evolution, natural optimized materials were obtained with outstanding mechanical performance surpassing that of many manufactured composites. These biomaterials exhibit exceptionally high tensile strength, hardness, and toughness characteristics. Among them, the amazing properties and structures of nacre have attracted great attention of researchers aiming to study and imitate its unique micro- and nanoscale architectures for the purpose of developing analogous artificial materials.[1−8] Although nacre-like composites have long been developed, the highly ordered structure and sophisticated building mechanisms in nacre have yet to be reproduced in artificial composites.[9] To better understand the structures and mechanical behaviors of biological materials, substantial models have been proposed.[10−14] Among them, a simple approach derived from a shear lag model,[15,16] based on the mechanics of the structures of natural composites, has been successfully applied to quantitatively explain the mechanical strength and ductility of nacre.[17] In this model, the applied load is transferred from the organic matrix to the inorganic platelets by shear stresses. According to this model, the operative failure mode determines the tensile strength of biological materials in terms of the aspect ratio of the inorganic platelets, s. For actual aspect ratios larger than the critical value ($s > s_c$), the composite fails under the platelet fracture mode, causing a fragile rupture of the composite. On the other hand, for actual aspect ratios smaller than the critical condition ($s < s_c$), the composite fails under the platelet pull-out mode, thus resulting in the continuous matrix and platelet−polymer interface yielding before the platelets break. In this shear lag mode, s_c is calculated as $s_c = \sigma_p/\tau_y$, where σ_p is the tensile strength of the inorganic platelet and τ_y is the matrix yield tensile strength. As a result, composites are strong but brittle and thus flaw-intolerant when failing under the platelet fracture mode, whereas materials are weak but ductile and thus flaw-tolerant when rupturing under the platelet pull-out mode. Therefore, if appropriate inorganic and organic materials with strong interfacial interactions in the pull-out mode are selected as reinforcing platelets and polymer components, bioinspired composites with both high strength and ductility will be fabricated.

Compared with other typical platelet-like inorganic materials, such as nanoclays,[18−20] glass flakes,[21] alumina flakes,[22,23] and graphene oxide,[24−28] the aspect ratio (s) of layered double hydroxide (LDH) nanosheets can be easily tuned during the synthesis process. Furthermore, combining their highly tunable properties with distinct anion-exchange properties, LDHs are regarded as a new emerging category of the most attractive inorganic material for fabricating artificial layered polymer/LDH composites with multiple functions.[29−35] Because of its water solubility, biodegradability, good chemical resistance, easy

Received: May 27, 2014
Accepted: August 20, 2014
Published: August 20, 2014

processability, and excellent mechanical properties, poly(vinyl alcohol) (PVA) is quite popular in many applications such as films, coatings, hydrogels, fibers, adhesives, and biomaterials.[36,37] Nevertheless, the insufficient mechanical properties of PVA limit its wide application. To date, many attempts have been made to fabricate PVA/LDH composites.[38−40] For instance, Ramaraj et al.[41] synthesized PVA/LDH nanocomposites in a solution-intercalation process for the first time. Their optical micrographs showed that the LDH sheets stacked and aggregated together with 2 wt % of LDH in the PVA/LDH nanocomposite, thus leading to the deterioration of the composite's mechanical properties. Huang et al.[42] prepared PVA/LDH composites directly with pristine LDH by the water solution-casting method. Hydrogen bonds could easily be formed between the hydroxyl groups of both LDH and PVA, so that the LDH uniformly dispersed in the aqueous PVA solution could interact with PVA firmly. Han et al.[43] prepared layered PVA/LDH films with improved mechanical properties using the layer-by-layer method. However, the mechanical properties of those PVA/LDH composites were far lower than predicted by theory. This resulted from the low fraction of inorganic platelets, poor dispersion, and random orientation of LDH nanosheets in the PVA matrix, as well as weak bonding at the inorganic−organic interface.

Hence, inspired by the hierarchical structure and excellent mechanical performance found in nacre, LDH platelets and PVA were chosen as rigid building blocks and polymer components for the fabrication of a strong and ductile bioinspired composite. With an estimated tensile strength (σ_p) of 2 GPa for the LDH nanoplatelets and a matrix yield tensile strength (τ_y) of ∼50 MPa for the PVA matrixes,[43] the s_c value of this material combination is 40. Under these conditions, uniform and hexagonal Co−Al CO_3 LDH platelets with an aspect ratio (s) of 19−37 (lateral size of 2−4 μm and thickness of 216.5 nm; $s \lesssim s_c$) were synthesized. The LDH platelets were designed with both a high aspect ratio to carry prominent loads and a small aspect ratio to permit rupture under the platelet pull-out mode. Therefore, these artificially synthesized LDH platelets were ideal candidates as two-dimensional inorganic building blocks for fabricating nacre-like PVA/LDH hybrid films that simultaneously exhibit both high tensile strength and ductility. Moreover, the large quantity of hydroxyl groups on the PVA molecules, as well as the hydroxyl and amino groups on the surface of pretreated LDH platelets, could facilitate the generation of hydrogen bonds intertwined at the organic−inorganic interface, increasing the adhesion between the inorganic platelets and the organic matrix. Multilayered PVA/LDH films were successfully prepared for the first time by bottom-up layer-by-layer assembly of pretreated LDH nanosheets and spin-coating of PVA (Scheme 1). The weight fraction of LDH platelets in the hybrid PVA/LDH films (w_p) was controlled by varying the concentration of the aqueous PVA solution applied in the spin-coating process. The resulting films revealed that the LDH platelets were aligned in the film and that the well-organized hierarchical structure depended strongly on the interfacial interaction existing between the inorganic LDH platelets and PVA molecules. Among all of the films, the 2 wt % PVA/LDH film had a very high loading of LDHs, up to 96.9 wt %, which was very close to the value in natural nacre. The prepared PVA/LDH hybrid films exhibited a combination of high tensile strength and elastic modulus, which could be compared with those of nacre and lamellar bone.

Scheme 1. Fabrication of Artificial Multilayered PVA/LDH Hybrid Films[a]

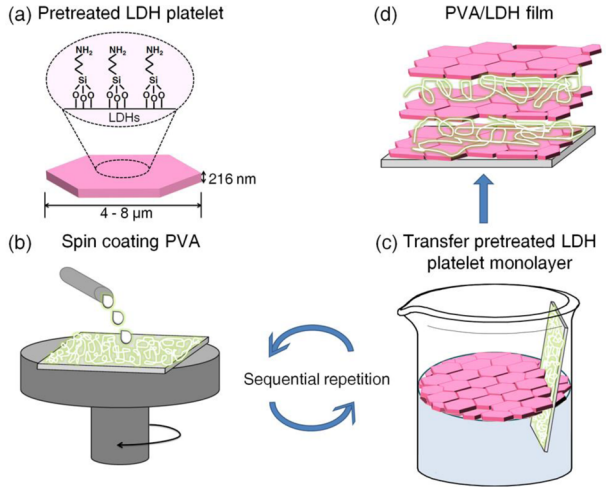

[a]Process steps: (a) modification of the surface of LDH platelets with slightly hydrophobic amine-terminated APTES; (b) spin coating of a layer of PVA onto the glass substrate; (c) slow addition of the pretreated LDH platelet suspension onto a water surface in a cylindrical beaker, resulting, after ultrasonication, in the gradual formation of a dense and homogeneous Langmuir film at the air−water interface, followed by transfer of the highly oriented monolayer of LDH platelets to the substrate with a polymer layer by manual dip coating; and (d) sequential repetition of steps b and c to fabricate multilayered PVA/LDH hybrid films.

EXPERIMENTAL SECTION

Materials. $CoCl_2{\cdot}6H_2O$, $AlCl_3{\cdot}6H_2O$, and CH_4N_2O were obtained from China Medicine Co. and used without further purification. The average polymerization degree of PVA, which was purchased from Beijing Yili Fine Chemicals Co., Ltd., was 1750. All other reagents were of analytical grade and were used without further purification.

Synthesis of LDH. Synthesis of CoAl−CO_3 LDH was based on a previous report[44] using a hydrolysis method.

Fabrication of PVA/LDH Nanocomposite Films. *Pretreatment of PVA.* PVA (1, 2, 3, or 4 g) was dissolved in deionized water (100 mL) under agitation, giving concentrations of 1, 2, 3, and 4 wt %.

Pretreatment of LDH Platelets. The platelets were surface modified with 3-aminopropyltriethoxysilane (APTES) as in a previous relevant report.[8,9]

Fabrication of Nacre-Like PVA/LDH Hybrid Films in Accordance with Refs 8 and 9. (i) In a typical procedure, a PVA layer was prepared by spin coating on a 2.4 cm × 2.4 cm glass substrate with PVA solution (1, 2, 3, or 4 wt %) at 1000 rpm for 1 min and then dried at 50 °C. (ii) Slowly dropping the solution of pretreated LDH platelets onto the water−air surface in a beaker until a new visible monolayer emerged. Then, after 15 min of ultrasonication, a homogeneous and dense film formed at the air−water interface. (iii) After these two steps were finished, the monolayer LDH film at the air−water interface was transferred to the glass substrate with one layer of PVA by careful manual dip coating. Then, the film was dried at 50 °C. Nacre-like hybrid PVA/LDH films were prepared through the sequential precipitation of organic and inorganic laminates on the substrate. Typical films were made up of 20 layers of inorganic LDH platelets, the first and last layers of which were generally deposited with PVA. The weight fraction of platelets in the hybrid film (w_p) was varied by controlling the concentration of PVA used in the spin-coating process.

Characterization. X-ray diffraction (XRD) patterns of the PVA/LDH films were obtained on a Shimadzu XRD-6000 diffractometer with Cu Kα radiation (λ = 0.1548 nm) under a voltage of 40 kV and a current of 40 mA. The morphologies of the samples were examined with a Hitachi S4800 scanning electron microscope, operated at an

accelerating voltage of 5 kV. A Bruker atomic force microscopy (AFM) system was utilized to detect the surface topography of the samples. UV−vis absorption spectra were recorded from 200 to 800 nm on a Shimadzu-3600 spectrophotometer equipped with a 1.0-nm-wide slit. Fourier transform infrared (FTIR) spectra were collected on a Nicolet iN10 infrared spectrophotometer. The mechanical properties of the films were measured on a Shimadzu AGS-X mechanical testing machine in the tensile mode. The tested samples were cut into a 25 mm × 3 mm rectangular shape, whose dimensions were determined precisely by scanning electron microscopy (SEM). The samples were stretched at a speed of 5 mm min^{-1}. The tensile properties reported here represent mean values of at least five samples' results.

RESULTS AND DISCUSSION

Highly crystalline and monodisperse CoAl−CO_3 LDH samples were prepared by the urea hydrolysis method under hydrothermal treatment. Figure 1a shows the XRD pattern of the

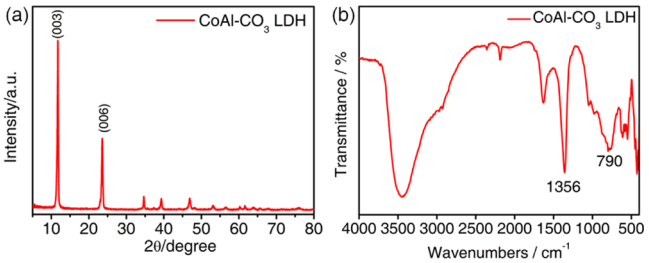

Figure 1. (a) XRD pattern of a CoAl−CO_3 LDH sample. (b) FTIR spectrum of the as-prepared CoAl−CO_3 LDH sample.

pink CoAl−CO_3 LDH powder. From this pattern, the parallel spacing of the LDH crystal plane was estimated to be about 0.75 nm due to incorporation of CO_3^{2-} in the interlayer of LDH.[45,46] According to the values for well-known LDH materials in CO_3^{2-} form,[45,46] all of the diffraction peaks of the prepared CoAl−CO_3 LDH could be considered as a rhombohedral structure. No impurity peaks were identified, demonstrating a completely pure phase. Moreover, the pointed and symmetric diffraction peaks strongly suggest that the CoAl−CO_3 LDH was highly crystallized. FTIR spectra (Figure 1b) of the as-prepared CoAl−CO_3 LDH provided evidence for the existence of intercalated CO_3^{2-} as well as water molecules. The strong peaks at 1356 and 790 cm^{-1} belong to the ν_3 vibration and bending modes, respectively, of CO_3^{2-}.[45] The broad band centered at 3450 cm^{-1} was assigned to the O−H stretching modes of interlayer water molecules and of H-bonded OH groups. The presence of a shoulder at around 3080 cm^{-1} suggests that the water molecules were H-bonded to CO_3^{2-} in the interlayer.

SEM images of the as-prepared CoAl−CO_3 LDH are shown in Figure 2a,b. As can be seen, the samples were well-crystallized into uniform and hexagonal platelets with an average lateral size of 2−4 μm. The as-prepared CoAl−CO_3 LDH was of high quality in many aspects including size, crystallinity, and morphology, as a result of the homogeneous nucleation procedure by gentle hydrolysis of urea. The thickness of the exfoliated nanosheet was examined by AFM. A tapping-mode AFM image (Figure 2c) showed that the lateral dimension of the two-dimensional LDH platelet was 4 μm. The height profile (Figure 2d) revealed that an individual LDH sheet had a considerably flat terrace with an average thickness of 216.5 nm. Hence, highly crystalline CoAl−CO_3 LDH nanosheets with aspect ratios (s) of 19−37 were

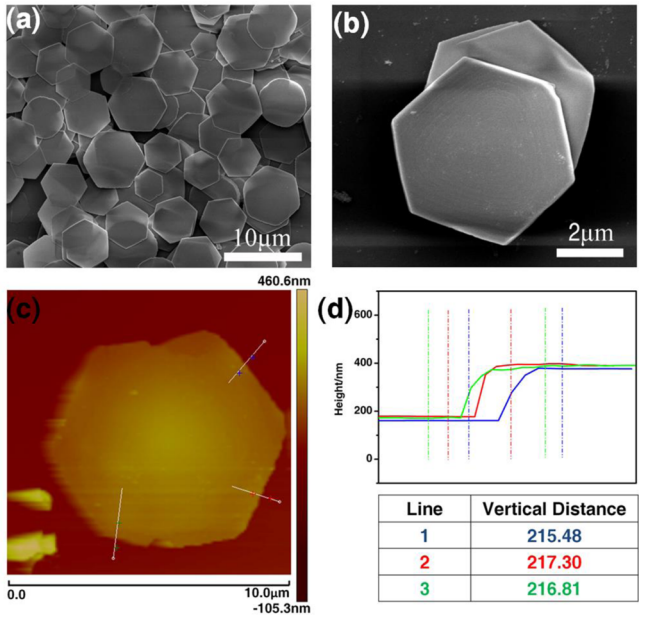

Line	Vertical Distance
1	215.48
2	217.30
3	216.81

Figure 2. (a) Low- and (b) high-magnification SEM images of a CoAl−CO_3 LDH sample. (c,d) Tapping-mode AFM (c) image and (d) height data of CoAl−CO_3 LDH nanosheets deposited on a silicon substrate.

considered as inorganic building blocks for fabricating bioinspired films. The aspect of the LDH nanosheets ($s < s_c$) determined the failure of the composite to be under the platelet pull-out mode.

As can be seen in Figure 3a, the PVA/LDH films were flexible, smooth, and glossy. The high concentration of PVA resulted in good dispersion of the LDH nanosheets, which decreased light scattering. Hence, the transmittance of the films gradually decreased with increasing LDH content. The cross sections of the PVA/LDH films (Figure 3b−e) revealed a well-defined layered architecture. The PVA/LDH hybrid films were analogous to the brick-and-mortar structure of nacre, because the inorganic building blocks of LDHs were piled close together. The platelet weight fraction (w_p) was affected by the PVA concentration used in the spin-coating process. A low concentration of PVA resulted in thin organic layers and a high inorganic fraction of LDH platelets in the 1 and 2 wt % PVA/LDH films, as shown in the SEM images (Figure 3b,c). The LDH platelets were clearly aligned parallel to the film surface and interpenetrated into the organic layers nearby, and the PVA served as a glue to interact with the platelets, as can be seen from the SEM images in Figure 3b,c. In contrast, for high PVA concentrations (low LDH platelet fractions), it can be seen that the LDH platelets were finely dispersed and homogeneously inlayed in the PVA matrix, as shown in Figure 3d,e. The inorganic−organic interfaces became vague with the increase in PVA concentration. Hence, PVA solutions with varied concentrations used during spin-coating could lead to significant differences in the cross-sectional morphologies of the resulting PVA/LDH films.

XRD patterns (Figure 4a) of the PVA/LDH films were collected with the purpose of studying the periodic structure. From the XRD patterns of the PVA/LDH films fabricated with different LDH loadings, the intrinsic layered symmetry of CoAl−CO_3 LDH in the hybrid films was still retained. Meanwhile, the characteristic peak of the PVA/LDH films

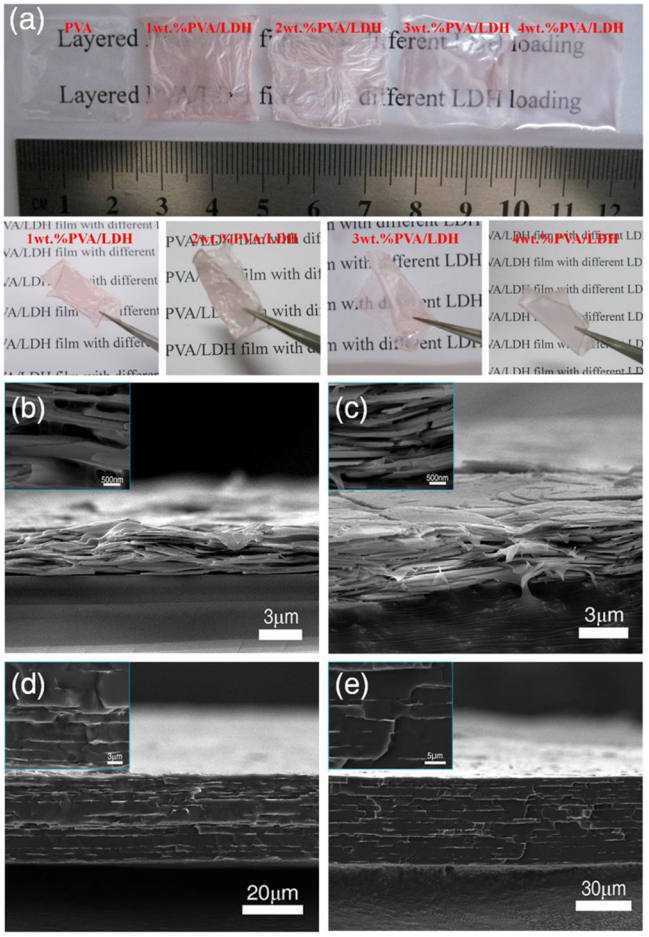

Figure 3. (a) Photographs of PVA/LDH films with different LDH contents. (b–e) SEM images of the cross sections of (b) 1, (c) 2, (d) 3, and (e) 4 wt % PVA/LDH films.

appeared at ca. 2.6° (Figure 4b), and the peak intensity increased with increasing LDH loading, indicating a long-range-ordered periodic structure along the normal direction of the layer plane, as well as a layer thickness of 3.4 nm. From the FTIR spectrum of the pristine PVA film (Figure 4c), the band between 3500 and 3200 cm^{-1} can clearly be ascribed to the O–H stretching vibration of free hydroxyl groups.[47] The peaks located at 2940 and 2905 cm^{-1} were attributed to $-CH_2-$ asymmetric and symmetric stretching, whereas the peaks corresponding to the bending and rocking of C–H groups were located at 1427 and 1328 cm^{-1}, respectively. When the concentration of the PVA solution was varied during the spin-coating procedure, the proportion of LDH platelets in the hybrid PVA/LDH films (w_p) changed accordingly. In the case of the PVA/LDH films, the characteristic absorption peaks centered at 1092 and 845 cm^{-1}, assigned to the stretching vibrations of C–OH and C–O, respectively,[48] were consistent with the pure PVA film. The strong peaks at 1356 and 790 cm^{-1} belong to the CO_3^{2-} groups of the LDH,[45] which was also obtained after the assembly. Further observation revealed that the PVA contents in the 4 and 3 wt % PVA/LDH films were greater than those in the 2 and 1 wt % PVA/LDH films, leading to obvious peaks of PVA. Similarly, the peaks intensities of LDH in the 2 and 1 wt % PVA/LDH films were more prominent than those in the other films. When the PVA/LDH films were compared with pure PVA film, however, it could be clearly seen that the original adsorption peak at 3344 cm^{-1} for the –OH stretching vibration in pure PVA moved to lower wavenumber at 3298 cm^{-1} in the PVA/LDH films with different LDH loadings. The variation associated with the –OH stretching vibration is forceful confirmation that hydrogen bonds were formed between PVA and LDH.[20] The large quantity of hydroxyl groups in the PVA molecules as well as the hydroxyl and amino groups on the surface of the pretreated LDH platelets could facilitate the generation of hydrogen bonds intertwined at the organic–inorganic interface, resulting in broader O–H bands.[49,50] Interestingly, with higher contents of inorganic LDH in the films, ranging from the 4 wt % PVA/LDH film to the 2 wt % PVA/LDH film, the peak intensity of the hydrogen bonding gradually increased. However, excess

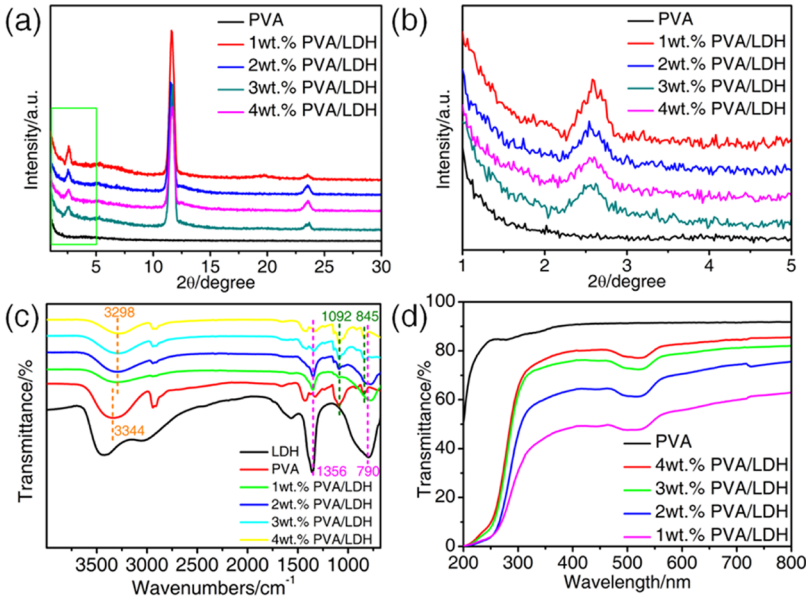

Figure 4. (a) XRD patterns of PVA/LDH films with different LDH contents and (b) close-up of the spectra in panel a. (c) FTIR spectra of LDH, PVA, and PVA/LDH films. (d) Light transmittance characteristics of PVA/LDH films with different LDH contents.

inorganic LDH nanosheets and insufficient PVA in the films could result in weak hydrogen bonding, such as in the 1 wt % PVA/LDH film. Thus, the appropriate contents of inorganic LDH and PVA in the 2 wt % PVA/LDH film could produce stronger interfacial interactions than those with either excess LDH or PVA. Light transmittance measurements showed that the transparencies of the PVA/LDH films were between 50% and 80% in the visible range, whereas for the pure PVA film, the value was found to be about 90% (Figure 4d). The light transmittance of the PVA/LDH films gradually decreased with increasing LDH content by lowering the concentration of PVA due to the light scattering effect of the LDH nanoplatelets. High transparencies were basically maintained by the 3 and 4 wt % PVA/LDH films. The 1 and 2 wt % PVA/LDH films exhibited obviously lower transparencies, because of their higher inorganic contents of LDH nanoplatelets compared to the 3 and 4 wt % PVA/LDH films.

The TGA curves of pure LDH, PVA, and PVA/LDH films with various LDH loadings are illustrated in Figure 5. For pure

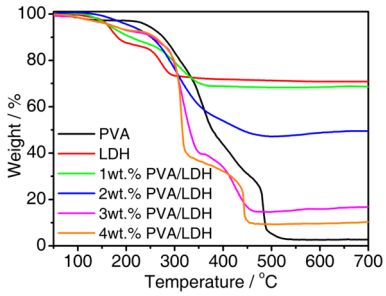

Figure 5. TGA comparison of LDH, PVA, and various PVA/LDH films.

LDH, the temperature for removal of interlayer water molecules and CO_2 (from intercalated CO_3^{2-}) was below 200 °C, which was assigned to the first stage of weight loss. The second stage of weight loss can be ascribed to the thermal decomposition of brucite-like layers through the removal of OH groups as water molecules. The residue of LDH was 70.5%. For pure PVA, the weight loss mainly occurred at temperatures ranging from 220 to 500 °C, leaving a residue that was merely about 2%. The first stage of PVA degradation was elimination of volatile products (the main product was water), during which the degradation rate became very high after 221 °C. Then, a large production of volatiles accompanied by the random scission of PVA molecular chains occurred, which led to a 90% weight loss of PVA before 500 °C.[51] The TGA curves of the PVA/LDH films showed three stages of weight loss, which were assigned to absorbed water evaporation, PVA and LDH degradation, and PVA backbone cleavage.[38] Obviously, all of the PVA/LDH films had higher decomposition rates and lower residues than the pure PVA film in the first two stages, ranging from 50 to 360 °C. Moreover, owing to the greater amounts of LDH in the 2 and 1 wt % PVA/LDH films, a multilayered carbonaceous structure was formed, effectively insulating the underlying materials and slowing the escape of volatile products generated during decomposition, so that the decomposition rates were lower and the residues were higher than those of the neat PVA film in the third stage. All PVA/LDH films showed higher residues than neat PVA. The residues were 68.8%, 49.5%, 16.5%, and 10% for the 1, 2, 3, and 4 wt % PVA/LDH films, respectively. From these data, the inorganic LDH loadings (w_p) of the 1, 2, 3, and 4 wt % PVA/LDH films could be calculated as 96.9%, 69.7%, 23.2%, and 14.1%, respectively. The temperature for 5% weight loss was regarded as the initial degradation temperature,[51] which was defined as T_{onset}. It can be seen that the T_{onset} values of the PVA/LDH films moved to lower temperatures than that of pure PVA (T_{onset} = 245 °C). With increasing content of LDH in the PVA matrix, T_{onset} was observed to be 174, 172, 205, and 164 °C for the 4, 3, 2, and 1 wt % PVA/LDH films, respectively. It can be clearly observed that the PVA/LDH hybrid films had worse thermal stability than pure PVA because of the addition of LDH in the composites. As shown in previous reports, LDH has been widely studied as catalysts.[52] In addition, similar phenomena were reported[42,53] as the explanation for the decreased thermal stability of PVA/LDH films, which could be attributed to the presence of Co and/or Al metals in LDH, the decomposition of PVA, and the subsequent reduction of the degradation temperature. However, the T_{onset} value of the 2 wt % PVA/LDH film was higher than those of the other films with different LDH contents. The primary reason for the 2 wt % PVA/LDH film exhibiting better thermal stability than the other films was the appropriate contents of inorganic LDH and PVA in the film, which could produce stronger interfacial interactions than those with either excess LDH or excess PVA. Therefore, the thermal stabilities decreased in the following order: PVA > 2 wt % PVA/LDH film > 4 wt % PVA/LDH film > 3 wt % PVA/LDH film > 1 wt % PVA/LDH film.

Representative stress−strain curves of neat PVA and PVA/LDH films are given in Figure 6. Compared with those of pure PVA, the mechanical properties of the PVA/LDH films were markedly enhanced. The pure PVA film had an initial elastic deformation followed by a large plastic deformation, with a tensile strength of 40.08 MPa. The Young's modulus and strain at break were about 0.45 GPa and 327%, respectively. Upon the mixing of inorganic LDH platelets in the PVA matrix, the

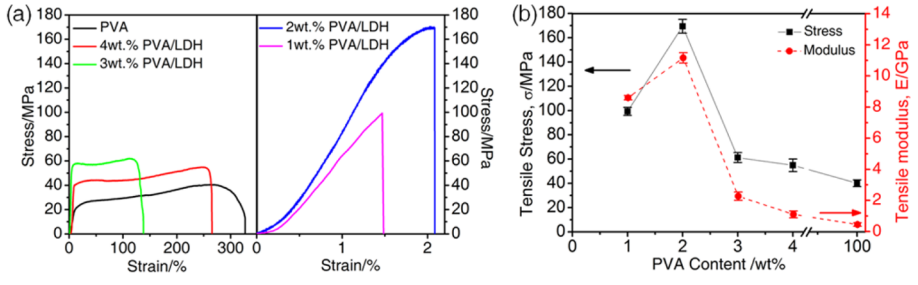

Figure 6. (a) Representative stress−strain curves of pure PVA and PVA/LDH films with different LDH weight fractions. (b) Tensile stress and tensile modulus of neat PVA and PVA/LDH films as functions of the PVA concentration in the films.

tensile strengths of the resulting PVA/LDH hybrid films were markedly enhanced with increasing LDH content. It could be perceived that the 4 and 3 wt % PVA/LDH films showed well-defined yield points and large plastic deformations. In contrast, as the LDH content continued to increase upon decreasing the PVA concentration to 2 and 1 wt %, the 2 and 1 wt % PVA/LDH films had much improved strengths, and neither yield nor plastic deformation was detected. Nevertheless, these PVA/LDH hybrid films became brittle, owing to the fact that the elongations at rupture gradually decreased with the augmentation of the LDH content in the films. The structures of the LDH platelets resembled those of nanoclay. As shown in previous reports,[54,55] clay−polymer composites are much more fragile than the corresponding pure polymer matrixes. Thus, it stands to reason that the hybrid films became brittle upon incorporating LDH into the PVA matrix. When the actual aspect ratio of the artificial LDH platelets was chosen to be less than the critical value, the stress and strain of the films could be maximized, and the films failed under the pull-out mode. Hence, compared with the catastrophic brittle fracture of natural nacre and other studies about composites containing clay platelets (with aspect ratios of >1000),[56−58] the 1 wt % PVA/LDH film with w_p = 96.9 wt % had a total break strain of 1.4%. From all of the analysis data above, it can be concluded that the LDH content plays an important role in the mechanical performance of PVA/LDH films. The tensile stress and tensile modulus at rupture as functions of PVA concentration (LDH content) were obtained, as shown in Figure 6b. It can be seen that the tensile stress and tensile modulus of these films increased as the LDH loading increased, whereas after reaching a maximum value, the tensile stress and modulus decreased with further incorporation of LDH. It is noteworthy that the tensile strength and the Young's modulus of the 2 wt % PVA/LDH films reached up to 169.36 MPa and 11.16 GPa, respectively. These values were 4.2 times and 24.8 times those of neat PVA, respectively. The tensile strength and strain at fracture of the obtained PVA/LDH films exceed the values obtained for nacre. Meanwhile, their elastic moduli could be compared with that of lamellar bone. However, the strength abruptly fell to 99.24 MPa as the LDH weight fraction increased to 96.9 wt % (1 wt % PVA/LDH).

The tensile fractured morphologies were observed by SEM to further investigate the mechanical properties of these PVA/LDH films. As shown in Figure 7a−d, cross sections of all of the fractured PVA/LDH films showed that the LDH platelets in the films were pulled out of the surrounding matrix but did not fracture under a tensile load. It can be clearly seen that pores formed around the inorganic LDH platelets, indicating the deboning of the LDH from the PVA matrix during the films' failure. The artificial LDH platelets with aspect ratios (s) of 19−37 could withstand higher loads and efficiently strengthened the films and, at the same time, ensured fracture under the pull-out mode because the s value of the LDH platelet was slightly smaller than s_c. The 4 and 3 wt % PVA/LDH films exhibited a brick-and-mortar architecture with ordered LDH platelets enveloped by the PVA matrix. Hence, the hybrid films would generate massive plastic deformation when the yield tensile strength of PVA was achieved, followed by the yielding of the organic matrix between the LDH platelets of the hybrid films. Meanwhile, voids were formed within the organic PVA matrix (Figure 7a,b). The fractured surfaces became much rougher as the LDH content in the films was increased, in accordance with the tensile tests. The 2 and 1 wt % PVA/LDH films broke after elastic deformation without substantial plastic flow (Figure 7c,d). Isolated voids could be seen from the cross sections of the untested films (Figure 3b,c), which represented crack initiation in the PVA matrix and potential sites for load concentration. These voids facilitated the fracture of the composites without obvious plastic deformation. Compared with the 2 wt % PVA/LDH film, more misalignment and pores appeared in the 1 wt % PVA/LDH film, which would prohibit the conduction of stress from the flexible organic matrix to the rigid LDH platelets and result in the reduction of both the yield strength and the elastic modulus of the hybrid films. The polymer with low concentration tended to form a very thin layer in the spin-coating process so as to achieve a high content of LDH. As previous reported,[16] the thin polymer layer could not even out the inorganic layers contiguous with the inherent small roughness of LDH platelets. Although all of the PVA/LDH films fractured under the pull-out mode, differences in the interfacial strength had a great impact on the mechanic properties of the PVA/LDH hybrid films. Obvious evidence was proposed to confirm the fact that hydrogen bonds existed between PVA and LDH by FTIR spectroscopy. Originating from the strong interfacial bonding between the LDH platelets and the PVA, the load could be efficiently transferred from the flexible polymer to the rigid inorganic building blocks. Among the PVA/LDH films with different LDH contents, the 2 wt % PVA/LDH film had an optimum ratio between LDH and PVA, which resulted in the strongest platelet−polymer interfacial strength. This is why the 2 wt % PVA/LDH film exhibited the best mechanical properties. These as-prepared LDH/PVA hybrid films exhibited a higher strength and ductility than those of analogous natural materials. The elastic moduli of the fabricated PVA/LDH films were still lower than the value for nacre. Therefore, it is still a challenge to eliminate the incorporation of defects completely in artificial hybrid films with a high content of inorganic platelets.

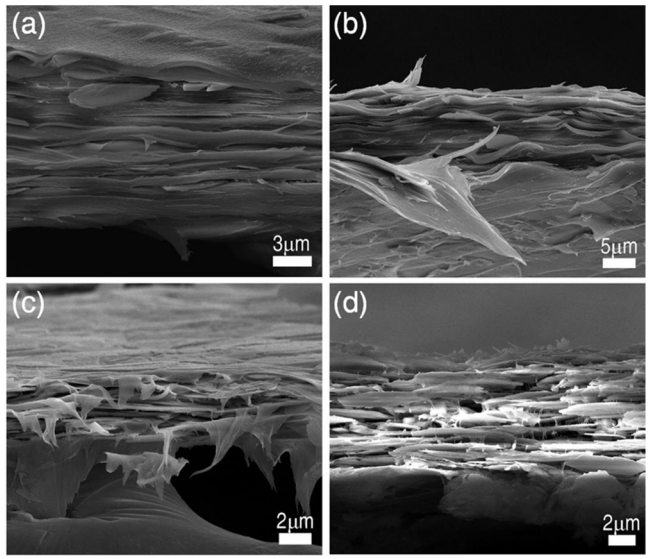

Figure 7. SEM images of (a) 4, (b) 3, (c) 2, and (d) 1 wt % PVA/LDH films after mechanical testing and film failure.

CONCLUSIONS

Nacre-liked hybrid films consisting of LDH platelets with an appropriate aspect ratio and PVA have been fabricated for the

first time. Amine groups at the end of the silane hydrophobic tail as well as hydroxyl groups on the surface of LDH nanosheets could easily form hydrogen bonds with the hydroxyl groups of the PVA, improving the interfacial interaction between platelets and the surrounding organic matrix. The microstructures of these PVA/LDH hybrid films showed a bioinspired hierarchical architecture with enhanced mechanical performance. The tensile strength of the 2 wt % PVA/LDH hybrid film reached 169.36 MPa, which exceeds the strength of natural nacre and is 4 times that of the pure PVA film. The development of this bioinspired approach to fabricate LDH−polymer artificial composites ruptured under the platelet pull-out mode and to control the inorganic platelet concentrations in the composites could allow for manufactured hybrid materials with enhanced and tunable mechanical performances. However, nature still dominates the most prominent materials fabrication with particular structures that are made from a minor scale of inorganic building blocks. Further advances in this area might allow for the selection of optimized artificial building blocks to fabricate nacre-like materials with multifunctionality and tailored mechanical properties in the future.

AUTHOR INFORMATION

Corresponding Author

*E-mail: pgyin@buaa.edu.cn.

Author Contributions

The manuscript was written through contributions of all authors. All authors have given approval to the final version of the manuscript.

Notes

The authors declare no competing financial interest.

ACKNOWLEDGMENTS

This work was supported by the National Basic Research Program of China (2010CB934700) and the Doctoral Fund of Innovation of Beijing University of Technology.

REFERENCES

(1) Mayer, G. Rigid Biological Systems as Models for Synthetic Composites. *Science* **2005**, *310*, 1144−1147.
(2) Deville, S.; Saiz, E.; Nalla, R. K.; Tomsia, A. P. Freezing as a Path to Build Complex Composites. *Science* **2006**, *311*, 515−518.
(3) Podsiadlo, P.; Kaushik, A. K.; Arruda, E. M.; Waas, A. M.; Shim, B. S.; Xu, J. D.; Nandivada, H.; Pumplin, B. G.; Lahann, J.; Ramamoorthy, A.; Kotov, N. A. Ultrastrong and Stiff Layered Polymer Nanocomposites. *Science* **2007**, *318*, 80−83.
(4) Munch, E.; Launey, M. E.; Alsem, D. H.; Saiz, E.; Tomsia, A. P.; Ritchie, R. O. Tough, Bio-Inspired Hybrid Materials. *Science* **2008**, *322*, 1516−1520.
(5) Tang, Z. Y.; Kotov, N. A.; Magonov, S.; Ozturk, B. Nanostructured Artificial Nacre. *Nature* **2003**, *2*, 413−418.
(6) Walther, A.; Bjurhager, I.; Malho, J. M.; Ruokolainen, J.; Berglund, L.; Ikkala, O. Supramolecular Control of Stiffness and Strength in Lightweight High-Performance Nacre-Mimetic Paper with Fire-Shielding Properties. *Angew. Chem., Int. Ed.* **2010**, *49*, 6448−6453.
(7) Walther, A.; Bjurhager, I.; Malho, J. M.; Pere, J.; Ruokolainen, J.; Berglund, L. A.; Ikkala, O. Large-Area, Lightweight and Thick Biomimetic Composites with Superior Material Properties via Fast, Economic, and Green Pathways. *Nano Lett.* **2010**, *10*, 2742−2748.
(8) Yao, H. B.; Fang, H. Y.; Tan, Z. H.; Wu, L. H.; Yu, S. H. Biologically Inspired, Strong, Transparent, and Functional Layered Organic−Inorganic Hybrid Films. *Angew. Chem., Int. Ed.* **2010**, *49*, 2140−2145.
(9) Bonderer, L. J.; Studart, A. R.; Gauckler, L. J. Bioinspired Design and Assembly of Platelet Reinforced Polymer Films. *Science* **2008**, *319*, 1069−1073.
(10) Jager, I.; Fratzl, P. Mineralized Collagen Fibrils: A Mechanical Model with a Staggered Arrangement of Mineral Particles. *Biophys. J.* **2000**, *79*, 1737−1746.
(11) Wang, R. Z.; Suo, Z.; Evans, A. G.; Yao, N.; Aksay, I. A. Deformation Mechanisms in Nacre. *J. Mater. Res.* **2001**, *16*, 2485−2493.
(12) Tang, H.; Barthelat, F.; Espinosa, H. D. An Elasto-Viscoplastic Interface Model for Investigating the Constitutive Behavior of Nacre. *J. Mech. Phys. Solids* **2007**, *55*, 1410−1438.
(13) Espinosa, H. D.; Rim, J. E.; Barthelat, F.; Buehler, M. J. Merger of Structure and Material in Nacre and Bone—Perspectives on *de Novo* Biomimetic Materials. *Prog. Mater. Sci.* **2009**, *54*, 1059−1100.
(14) Evans, A. G.; Suo, Z.; Wang, R. Z.; Aksay, I. A.; He, M. Y.; Hutchinson, J. W. Model for the Robust Mechanical Behavior of Nacre. *J. Mater. Res.* **2001**, *16*, 2475−2484.
(15) B. Glavinchevski, M. P. Steel Disc Reinforced Polycarbonate. *J. Mater. Sci.* **1973**, *8*, 1373−1382.
(16) Bonderer, L. J.; Studart, A. R.; Woltersdorf, J.; Pippel, E.; Gauckler, L. J. Strong and Ductile Platelet-Reinforced Polymer Films Inspired by Nature: Microstructure and Mechanical Properties. *J. Mater. Res.* **2009**, *24*, 2741−2754.
(17) Jackson, A. P.; Vincent, J. F. V.; Turner, R. M. The Mechanical Design of Nacre. *Proc. R. Soc. London B* **1988**, *234*, 415−440.
(18) Yao, H. B.; Tan, Z. H.; Fang, H. Y.; Yu, S. H. Artificial Nacre-like Bionanocomposite Films from the Self-Assembly of Chitosan−Montmorillonite Hybrid Building Blocks. *Angew. Chem., Int. Ed.* **2010**, *49*, 10127−10131.
(19) Wang, J. F.; Cheng, Q. F.; Lin, L.; Chen, L. F.; Jiang, L. Understanding the Relationship of Performance with Nanofiller Content in the Biomimetic Layered Nanocomposites. *Nanoscale* **2013**, *5*, 6356−6362.
(20) Podsiadlo, P.; Tang, Z. Y.; Shim, B. S.; Kotov, N. A. Counterintuitive Effect of Molecular Strength and Role of Molecular Rigidity on Mechanical Properties of Layer-by-Layer Assembled Nanocomposites. *Nano Lett.* **2007**, *7*, 1224−1231.
(21) Fu, Q.; Saiz, E.; Rahaman, M. N.; Tomsia, A. P. Toward Strong and Tough Glass and Ceramic Scaffolds for Bone Repair. *Adv. Funct. Mater.* **2013**, *23*, 5461−5476.
(22) Bonderer, L. J.; Feldman, K.; Gauckler, L. J. Platelet-Reinforced Polymer Matrix Composites by Combined Gel-Casting and Hot-Pressing. Part I: Polypropylene Matrix Composites. *Compos. Sci. Technol.* **2010**, *70*, 1958−1965.
(23) Bonderer, L. J.; Feldman, K.; Gauckler, L. J. Platelet-Reinforced Polymer Matrix Composites by Combined Gel-Casting and Hot-Pressing. Part II: Thermoplastic Polyurethane Matrix Composites. *Compos. Sci. Technol.* **2010**, *70*, 1966−1972.
(24) Cheng, Q. F.; Wu, M. X.; Li, M. Z.; Jiang, L.; Tang, Z. Y. Ultratough Artificial Nacre Based on Conjugated Cross-Linked Graphene Oxide. *Angew. Chem., Int. Ed.* **2013**, *52*, 3750−3755.
(25) Li, Y. Q.; Yu, T.; Yang, T. Y.; Zheng, L. X.; Liao, K. Bio-Inspired Nacre-like Composite Films Based on Graphene with Superior Mechanical, Electrical, and Biocompatible Properties. *Adv. Mater.* **2012**, *24*, 3426−3431.
(26) Wang, X. L.; Bai, H.; Yao, Z. Y.; Liu, A. R.; Shi, G. Q. Electrically Conductive and Mechanically Strong Biomimetic Chitosan/Reduced Graphene Oxide Composite Films. *J. Mater. Chem.* **2010**, *20*, 9032−9036.
(27) Kakisawa, H.; Sumitomo, T.; Inoue, R.; Kagawa, Y. Fabrication of Nature-Inspired Bulk Laminar Composites by a Powder Processing. *Compos. Sci. Technol.* **2010**, *70*, 161−166.
(28) Zhong, D.; Yang, Q. L.; Guo, L.; Dou, S. X.; Liu, K. S.; Jiang, L. Fusion of Nacre, Mussel, and Lotus Leaf: Bio-Inspired Graphene Composite Paper with Multifunctional Integration. *Nanoscale* **2013**, *5*, 5758−5764.
(29) Dou, Y. B.; Xu, S. M.; Liu, X. X.; Han, J. B.; Yan, H.; Wei, M.; Evans, D. G.; Duan, X. Transparent, Flexible Films Based on Layered

Double Hydroxide/Cellulose Acetate with Excellent Oxygen Barrier Property. *Adv. Funct. Mater.* **2014**, *24*, 514−521.
(30) Zumreoglu-Karan, B.; Ay, A. N. Layered Double Hydroxides—Multifunctional Nanomaterials. *Chem. Pap.* **2012**, *66*, 1−10.
(31) Yan, D. P.; Lu, J.; Wei, M.; Li, S. D.; Evans, D. G.; Duan, X. Luminescent Ultrathin Film of Anionic Styrylbiphenyl Derivative−Layered Double Hydroxide and Its Reversible Sensing for Heavy Metal Ions. *Phys. Chem. Chem. Phys.* **2012**, *14*, 8591−8598.
(32) Yan, D. P.; Lu, J.; Wei, M.; Qin, S. H.; Chen, L.; Zhang, S. T.; Evans, D. G.; Duan, X. Heterogeneous Transparent Ultrathin Films with Tunable-Color Luminescence Based on the Assembly of Photoactive Organic Molecules and Layered Double Hydroxides. *Adv. Funct. Mater.* **2011**, *21*, 2497−2505.
(33) Yan, D. P.; Lu, J.; Ma, J.; Wei, M.; Evans, D. G.; Duan, X. Reversibly Thermochromic, Fluorescent Ultrathin Films with a Supramolecular Architecture. *Angew. Chem., Int. Ed.* **2011**, *50*, 720−723.
(34) Shu, Y. Q.; Yin, P. G.; Liang, B. L.; Wang, S. S.; Gao, L. C.; Wang, H.; Guo, L. Layer by Layer Assembly of Heparin/Layered Double Hydroxide Completely Renewable Ultrathin Films with Enhanced Strength and Blood Compatibility. *J. Mater. Chem.* **2012**, *22*, 21667−21672.
(35) Shu, Y. Q.; Yin, P. G.; Wang, J. F.; Liang, B. L.; Wang, H.; Guo, L. Bioinspired Nacre-like Heparin/Layered Double Hydroxide Film with Superior Mechanical, Fire-Shielding, and UV-Blocking Properties. *Ind. Eng. Chem. Res.* **2014**, *53*, 3820−3826.
(36) Krumova, M.; Lopez, D.; Benavente, R.; Mijangos, C.; Perena, J. M. Effect of Crosslinking on the Mechanical and Thermal Properties of Poly(vinyl alcohol). *Polymer* **2000**, *41*, 9265−9272.
(37) Liu, L. Q.; Gao, Y.; Liu, Q.; Kuang, J.; Zhou, D.; Ju, S. T.; Han, B. H.; Zhang, Z. High Mechanical Performance of Layered Graphene Oxide/Poly(vinyl alcohol) Nanocomposite Films. *Small* **2013**, *9*, 2466−2472.
(38) Zeng, L.; Zhao, T. S.; Li, Y. S. Synthesis and Characterization of Crosslinked Poly(vinyl alcohol)/Layered Double Hydroxide Composite Polymer Membranes for Alkaline Direct Ethanol Cells. *Int. J. Hydrogen Energy* **2012**, *37*, 18425−18432.
(39) Huang, S.; Yang, Z.; Zhu, H.; Ren, L. L.; Tjiu, W. W.; Liu, T. X. Poly(vinly alcohol)/Nano-Sized Layered Double Hydroxides Nanocomposite Hydrogels Prepared by Cyclic Freezing and Thawing. *Macromol. Res.* **2012**, *20*, 568−577.
(40) Zhao, L. N.; Yang, D. Y.; Dong, M. D.; Xu, T.; Jin, Y.; Xu, S. L.; Zhang, F. Z.; Evans, D. G.; Jiang, X. Y. Fabrication and Wettability of Colloidal Layered Double Hydroxide-Containing PVA Electrospun Nanofibrous Mats. *Ind. Eng. Chem. Res.* **2010**, *49*, 5610−5615.
(41) Ramaraj, B.; Nayak, S. K.; Yoon, K. R. Poly(vinyl alcohol) and Layered Double Hydroxide Composites: Thermal and Mechanical Properties. *J. Appl. Polym. Sci.* **2010**, *116*, 1671−1677.
(42) Huang, S.; Cen, X.; Zhu, H.; Yang, Z.; Yang, Y.; Tjiu, W. W.; Liu, T. X. Facile Preparation of Poly(vinyl alcohol) Nanocomposites with Pristine Layered Double Hydroxides. *Mater. Chem. Phys.* **2011**, *130*, 890−896.
(43) Han, J. B.; Dou, Y. B.; Yan, D. P.; Ma, J.; Wei, M.; Evans, D. G.; Duan, X. Biomimetic Design and Assembly of Organic−Inorganic Composite Films with Simultaneously Enhanced Strength and Toughness. *Chem. Commun.* **2011**, *47*, 5274−5276.
(44) Huang, S.; Cen, X.; Peng, H. D.; Guo, S. Z.; Wang, W. Z.; Liu, T. X. Heterogeneous Ultrathin Films of Poly(vinyl alcohol)/Layered Double Hydroxide and Montmorillonite Nanosheets via Layer-by-Layer Assembly. *J. Phys. Chem. B* **2009**, *113*, 15225−15230.
(45) Liu, Z. P.; Ma, R. Z.; Osada, M.; Iyi, N.; Ebina, Y.; Takada, K.; Sasaki, T. Synthesis, Anion Exchange, and Delamination of Co−Al Layered Double Hydroxide: Assembly of the Exfoliated Nanosheet/Polyanion Composite Films and Magneto-Optical Studies. *J. Am. Chem. Soc.* **2006**, *128*, 4872−4880.
(46) Zhu, H.; Huang, S.; Yang, Z.; Liu, T. X. Oriented Printable Layered Double Hydroxide Thin Films via Facile Filtration. *J. Mater. Chem.* **2011**, *21*, 2950−2956.
(47) Qin, X. H.; Wang, S. Y. Electrospun Nanofibers from Crosslinked Poly(vinyl alcohol) and Its Filtration Efficiency. *J. Appl. Polym. Sci.* **2008**, *109*, 951−956.
(48) Zhao, G. H.; Liu, Y.; Fang, C. L.; Zhang, M.; Zhou, C. Q.; Chen, Z. D. Water Resistance, Mechanical Properties and Biodegradability of Methylated-Cornstarch/Poly(vinyl alcohol) Blend Film. *Polym. Degrad. Stab.* **2006**, *91*, 703−711.
(49) Perez-Bernal, M. E.; Ruano-Casero, R. J.; Benito, F.; Rives, V. Nickel−Aluminum Layered Double Hydroxides Prepared via Inverse Micelles Formation. *J. Solid State Chem.* **2009**, *182*, 1593−1601.
(50) Tang, Z. Y.; Wang, Y.; Podsiadlo, P.; Kotov, N. A. Biomedical Applications of Layer-by-Layer Assembly: From Biomimetics to Tissue Engineering. *Adv. Mater.* **2006**, *18*, 3203−3224.
(51) Zhao, C. X.; Liu, Y.; Wang, D. Y.; Wang, D. L.; Wang, Y. Z. Synergistic Effect of Ammonium Polyphosphate and Layered Double Hydroxide on Flame Retardant Properties of Poly(vinyl alcohol). *Polym. Degrad. Stab.* **2008**, *93*, 1323−1331.
(52) Choudary, B. M.; Madhi, S.; Chowdari, N. S.; Kantam, M. L.; Sreedhar, B. Layered Double Hydroxide Supported Nanopalladium Catalyst for Heck-, Suzuki-, Sonogashira-, and Stille-Type Coupling Reactions of Chloroarenes. *J. Am. Chem. Soc.* **2002**, *124*, 14127−14136.
(53) Chiang, M. F.; Wu, T. M. Synthesis and Characterization of Biodegradable Poly(L-lactide)/Layered Double Hydroxide Nanocomposites. *Compos. Sci. Technol.* **2010**, *70*, 110−115.
(54) Das, P.; Schipmann, S.; Malho, J. M.; Zhu, B. L.; Klemradt, U.; Walther, A. Facile Access to Large-Scale, Self-Assembled, Nacre-Inspired, High-Performance Materials with Tunable Nanoscale Periodicities. *ACS Appl. Mater. Interfaces* **2013**, *5*, 3738−3747.
(55) Sehaqui, H.; Kochumalayil, J.; Liu, A. D.; Zimmermann, T.; Berglund, L. A. Multifunctional Nanoclay Hybrids of High Toughness, Thermal, and Barrier Performances. *ACS Appl. Mater. Interfaces* **2013**, *5*, 7613−7620.
(56) Podsiadlo, P.; Liu, Z. Q.; Paterson, D.; Messersmith, P. B.; Kotov, N. A. Fusion of Seashell Nacre and Marine Bioadhesive Analogs: High-Strength Nanocompoisite by Layer-by-Layer Assembly of Clay and L-3,4-Dihydroxyphenylalanine Polymer. *Adv. Mater.* **2007**, *19*, 949−955.
(57) Podsiadlo, P.; Kaushik, A. K.; Shim, B. S.; Agarwal, A.; Tang, Z. Y.; Waas, A. M.; Arruda, E. M.; Kotov, N. A. Can Nature's Design be Improved Upon? High Strength, Transparent Nacre-Like Nanocomposites with Double Network of Sacrificial Cross Links. *J. Phys. Chem. B* **2008**, *112*, 14359−14363.
(58) Podsiadlo, P.; Michel, M.; Critchley, K.; Srivastava, S.; Qin, M.; Lee, J. W.; Verploegen, E.; Hart, A. J.; Qi, Y.; Kotov, N. A. Diffusional Self-Organization in Exponential Layer-by-Layer Films with Micro- and Nanoscale Periodicity. *Angew. Chem., Int. Ed.* **2009**, *48*, 7073−7077.